Proceedings of the 5th World Congress on Momentum, Heat and Mass Transfer (MHMT'20)
~~Lisbon, Portugal~~ Virtual Congress – October 2020
Paper No. ENFHT 171
DOI: 10.11159/enfht20.171

Experimental Study on Evaporation properties during Spray Flash of Aqueous NaCl Solution

Huihui Wang, Dan Zhang*, Shuran Zhao, Jiping Liu
Xi'an Jiaotong University
710049, Xi'an, China
wang_hh@stu.xjtu.edu.cn; zhangdan@mail.xjtu.edu.cn

Abstract - In this paper, experimental study on evaporation properties under differential pressure (Δp, 0.1-1.5 MPa), superheat (ΔT, 0-22 K) mass fraction (f_m, 0-0.15) and injection distance (x, 21-31 mm) during spray flash of aqueous NaCl solution. The velocity field is measured by the high-speed camera and image registration. The droplet size is measured by Malvern Analyzer. Mainly found velocity increases with rising Δp or ΔT, and decreases with rising f_m. The droplet size decreases with rising Δp or x, and decreases with rising ΔT or f_m. On basis of these results, a one-calculation model for spray flash was set up. The evolution of droplet size/velocity/temperature could be well computed from given evolution of spray flash pressure and other necessary initial conditions.

***Keywords*:** spray flash; velocity flied; droplet size; evaporation properties.

1. Introduction

Flash defines suddenly boiling of superheated liquid induced by sudden pressure drop below its saturated pressure. According to the shape of superheated liquid, flash can be classified as film flash, droplet flash or spray flash. Spray flash was one of the effective methods to process salty wastewater with high concentration. Its advantages included no heating surface, larger interface intensity, smaller driving superheat and easily separation of generated crystal. This phenomenon is widely used for seawater desalination [1], concentration [2], surface cooling [3], atomization [4], and so on.

Miyatake et al. [5] defined superheat (ΔT) as the difference between initial waterfilm temperature and saturation temperature under final equilibrium pressure of flash chamber. Superheat represented the total unstable energy contained in waterfilm. Ikegami et al. [6] divide flow field into a liquid column, an atomization evaporation and saturation regions in spray flash. And indicated the upward spray method has the possibility of making the spray flash desalination system more compact and efficient. Araghi et al. [7] experimentally study on the vertical spray flash of 3.5% NaCl solution. The coupling relationship between the droplet size and velocity distribution and the thermodynamic characteristics such as temperature, superheat and concentration distribution was analysed. Our research group [8,9] uses the high-speed camera to observe the spray flash field, and the rapid measurement of the velocity field is realized through the image registration.

However, previous researches still have few limitations. The research is mainly on low-concentration NaCl solution. And the study was carried out in a vertical upward and downward spray. In this paper, aqueous NaCl solution was used as working fluid. The velocity field was measured by high speed camera and image registration technique. The droplet size was measured by Malvern, and a one-dimensional atomization evaporation model was established according to the experimental results. The research content of this paper provides a theoretical basis for the industrial application of high concentration spray flash and crystallization.

2. Experimental setup and uncertainty analysis

2. 1. Experimental setup

In this paper, experiments were carried out under differential pressure (Δp), superheat (ΔT) and mass fraction (f_m) of solution on basis of the experimental rig as shown in Fig.1. In experiments, aqueous NaCl solution with certain initial mass fraction was heated and pressed out by high pressure nitrogen. A stable spray flash was achieved through DANFOSS nozzle in test section. The typical flow field structure was shown in Fig.2.

2. 2. Uncertainty analysis

The experimental ranges of main parameters and their uncertainty analyses results are all listed in Table.1. Their uncertainties are evaluated according to method proposed by Moffat [10].

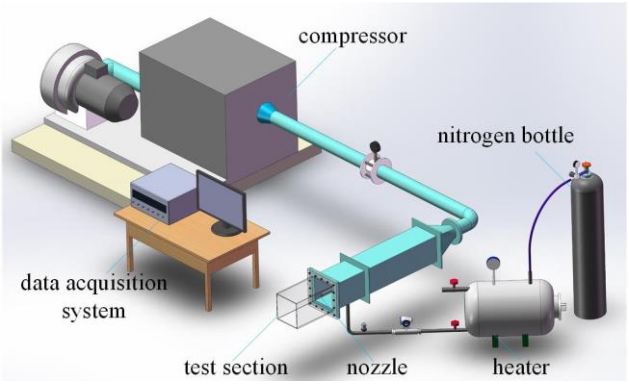

Fig. 1: Schematic of spray flash system.

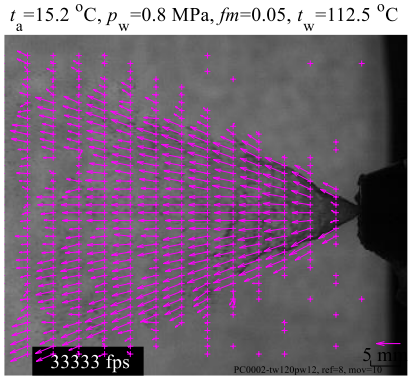

Fig. 2: Typical flow field structure.

Table 1: Uncertainty analysis.

Parameter	Measuring range [x_{min}-x_{max}]	Maximal uncertainty $\delta_{x,x}/x_{x,min}$
Δp / MPa	0.1-1.50	0.080
t_w / ℃	13-132.6	0.028
f_m	0-0.15	0.01
ΔT / K	0-23.5	0.039
x / mm	21-31	0.005
$\bar{V}$,u_d/ m·s^{-1}	13.2-57.61	-
D,D_{32} / μm	38-363	-

3. Results and discussion

3. 1. Mass flow

3. 1. Velocity field

The mean velocity of axial section ($\bar{V}$), calculated by Eq.(1), represents the diffused intensity. Fig.3 shows $\bar{V}$ increases with rising Δp or ΔT, and decreases with rising f_m. When there is superheat, $\bar{V}$ slightly increases and quickly decreases in the axial distance. It indicates droplet phase transition releases part of heat energy into kinetic energy. u_d is will be involved as a calculated value of $\bar{V}$.

$$\bar{V} = \frac{1}{n}\sum_{i=1}^{n}\sqrt{u_i^2 + v_i^2} \tag{1}$$

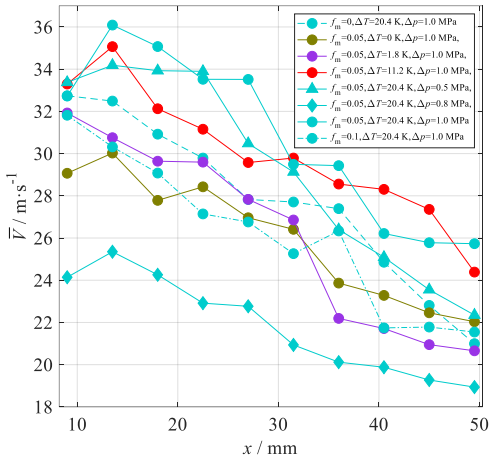

Fig. 3: Δp, ΔT and f_m vs. velocity.

3. 2. Droplet size

Using Malvern Analyzer measure droplets size in axial direction. Sauter mean diameter (D_{32}) indicate droplets size (D). The change of droplet size (D) reflects the evaporation intensity. Fig.4 shows the variation of D versus differential pressure in the axial distance. D decreases with rising Δp. Δp increases cause initial kinetic energy increases and thus affect D decreases. D decreases steeply first and then slowly with the x increases. This phenomenon is affected by evaporation.

Fig.5 and Fig.6 shows the variation of D versus superheat and mass fraction in the axial distance. The result is D increases with rising ΔT. When there is superheat, the mixing of steam and droplets in spray flash process increases droplet instability that cause D increases. The result is D increases with rising f_m. It indicates that f_m increases cause surface tension increases that affect D increases.

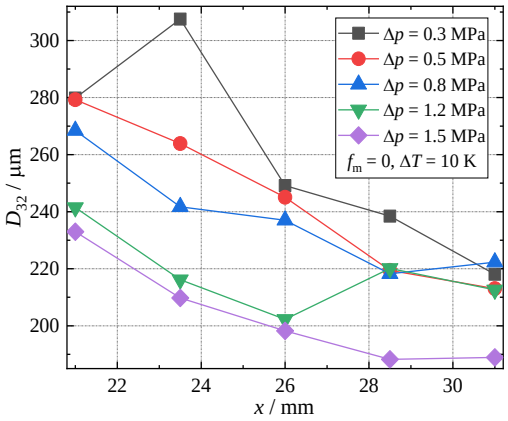

Fig. 4: Δp and x vs. droplet size.

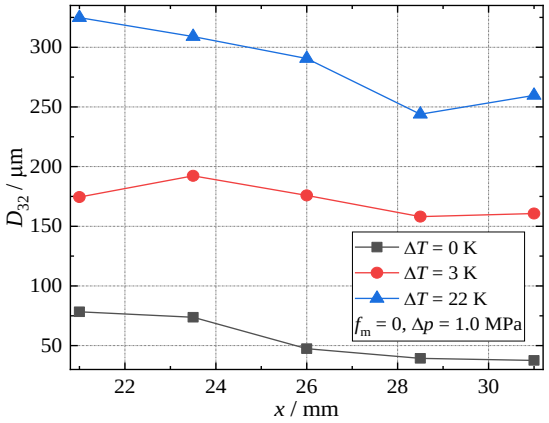

Fig. 5: ΔT and x vs. droplet size.

Fig. 6: f_m and x vs. droplet size.

4. Evaporation Model

4. 1. Model Establishment

In this model, the liquid-phase volume (V) of droplet at the current moment is selected as control part, and the control part is surrounded by a closed curved surface A. The main assumptions include:

a. The droplet size is only reduced by evaporation in stable evaporation concentration.

b. Vapour is calculated as ideal gas in spray flash.

c. The droplet size is measured as the true droplet size.

d. The change of density along the course is not taken into account.

The calculation principle is that variability of D is mainly by evaporation in stable evaporation concentration. Fig.7 shows typical process of spray flash along the injection direction.

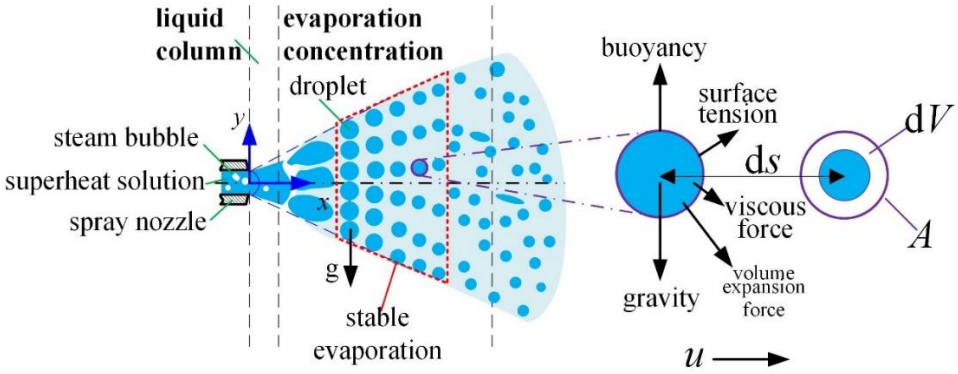

Fig. 7: Typical process of spray flash along the injection direction.

4. 2. Heat transfer properties

According to these variation rules, *Nu* further represents droplet surface evaporation intensity. It could is measured by Eq.(4) reshaped from Eq.(3) and Eq.(2).

$$h_s A\Delta T = \frac{h_{fg} m_w}{d\tau} \tag{2}$$

$$Nu = \frac{h_s D}{\lambda_d} \tag{3}$$

$$Nu = \frac{\rho_d r}{2(t_w - t_s)} \frac{D_{32}}{\lambda_d} \cdot \frac{dD}{dx} \cdot \frac{dx}{d\tau} \approx \frac{\rho_d r}{2\Delta T} \frac{D}{\lambda_d} \cdot \frac{\Delta D}{\Delta x} \cdot u_d \tag{4}$$

Re represents the movement characteristics of spray flash flow field. *Ja* represents the phase transition characteristics of spray flash. So *Nu* is fitted as Eq.(7). The relative error between experimental and calculated results is displayed in Fig.8.

$$Re = \frac{\rho_d D u_d}{\mu_d} \tag{5}$$

$$Ja = \frac{c_d \Delta T}{r} \tag{6}$$

$$Nu = 0.021 Re^{5.04} Ja^{-1.73} \tag{7}$$

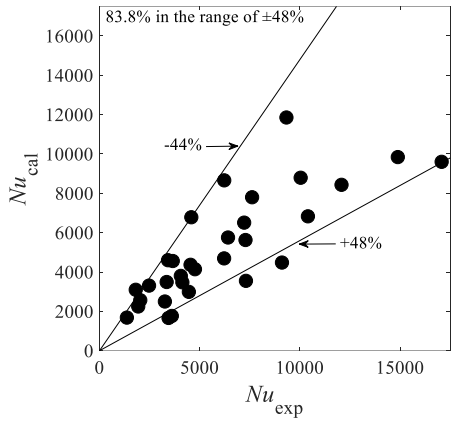

Fig. 8: Error distribution of *Nu*.

4. 3. One-dimensional evaporation model

4. 3. 1. Mass transfer

According to AN and HH, the continuity equation describes mass transfer in the spray flash of droplets.

$$\frac{\partial}{\partial \tau}\left[\alpha_{\mathrm{k}}\rho_{\mathrm{k}}\right]+\nabla\left[\alpha_{\mathrm{k}}\rho_{\mathrm{k}}\vec{u}_{\mathrm{k}}\right]=\Gamma_{\mathrm{k}} \tag{8}$$

in which α_{k} is regarded as the local k-phase time fraction. Γ_{k} represents the mass transfer rate of phase transition in unit of time.

Flash causes liquid evaporation to produce steam. So the basic differential equation of mass transfer is obtained:

$$\frac{\partial}{\partial \tau}\left[\alpha_{\mathrm{k}}\rho_{\mathrm{k}}\right]+\frac{\partial}{\partial r}\left[\alpha_{\mathrm{k}}\rho_{\mathrm{k}}u_{\mathrm{k}}\right]=\Gamma_{\mathrm{k}} \tag{9}$$

During phase transition process, the sensible heat carried by the initial droplet mass is converted into latent heat. The process is calculated by:

$$c_k\rho_k V\ \frac{\mathrm{d}t}{\mathrm{d}\tau}=\Gamma_k h_{\mathrm{L}} \tag{10}$$

The model contains two components: aqueous NaCl solution and steam. To simplify model and according to mass transfer rate (Γ_{k}) conservation phase transition, the mass conservation equation is given by:

$$\frac{\rho_{\mathrm{d}}\mathrm{d}V}{\mathrm{d}\tau}=\frac{\rho_{\mathrm{vap}}\mathrm{d}V}{\mathrm{d}\tau}+\rho_{\mathrm{vap}}u_{\mathrm{I}}A \tag{11}$$

in which u_{I} is regarded as steam diffusion velocity in the interface.

Then because u_{I} is difficult to measure, the steam diffusion mass approximately calculated by energy conservation.

$$\begin{cases} \dfrac{\mathrm{d}m_{\mathrm{I}}}{\mathrm{d}\tau} \approx \rho_{\mathrm{vap}} u_{\mathrm{I}} A \\ \dfrac{\mathrm{d}m_{\mathrm{I}}}{\mathrm{d}\tau} \approx \dfrac{h_{\mathrm{s}} A}{r} \dfrac{\mathrm{d}t_{\mathrm{d}}}{\mathrm{d}\tau} \end{cases} \tag{12}$$

in which m_{I} is regarded as steam diffusion mass. h_{s} is regarded as surface heat transfer coefficient and represents the transferred heat through per unit surface in per unit time. r is regarded as the latent heat of phase transition.

Geometric relationship of droplet mass transfer is given by:

$$\frac{\mathrm{d}V}{\mathrm{d}\tau} = \frac{\mathrm{d}}{\mathrm{d}\tau}\left(\frac{4}{3}\pi r^3\right) = \frac{\pi}{2} D^2 \frac{\mathrm{d}D}{\mathrm{d}\tau} \tag{13}$$

The droplet diameter is much larger than the average free path of water vapour in experimental range. Meanwhile $\rho_{\mathrm{d}} >> \rho_{\mathrm{vap}}$. Variation of droplet diameter with time is obtained based on Eqs.(11), (12) and (13):

$$\frac{\mathrm{d}D}{\mathrm{d}\tau} = \frac{2\left(1-f_{\mathrm{m}}\right) h_{\mathrm{s}}}{\rho_{\mathrm{w}} r} \frac{\mathrm{d}t_{\mathrm{d}}}{\mathrm{d}\tau} \tag{14}$$

4. 3. 2. Droplet movement model

Fig.9 illustrates the schematic of the force acting on the droplet. The droplet displacement equation and the momentum equation with phase transition is respectively expressed by:

$$\frac{\mathrm{d}x}{\mathrm{d}\tau} = u_{\mathrm{d}} \tag{15}$$

$$\frac{\partial}{\partial\tau}\left[\alpha_{\mathrm{k}}\rho_{\mathrm{k}}u_{\mathrm{k}}\right] + \vec{\nabla}\left[\alpha_{\mathrm{k}}\rho_{\mathrm{k}}u_{\mathrm{k}}u_{\mathrm{k}}\right] = -\vec{\nabla}\left(\alpha_{\mathrm{k}}p_{\mathrm{k}}\right) + \vec{\nabla}\left(\alpha_{\mathrm{k}}\mu_{\mathrm{k}}u_{\mathrm{k}}\right) + G_{\mathrm{k}} + \Gamma_{\mathrm{k}}u_{\mathrm{k}} - f_{\mathrm{D,k}} + \alpha_{\mathrm{k}}\rho_{\mathrm{k}}g_{\mathrm{k}} \tag{16}$$

$$C_{\mathrm{D}} = 0.534\left(\frac{0.263Re^{2.31} + 253.8Re^{0.52} + 6.33}{Re}\right) \tag{17}$$

where, $f_{\mathrm{D,k}} = \rho_{\mathrm{k}} C_{\mathrm{D}} u_{\mathrm{k}}^2 / 2$. G_{k} is regarded as expansion force per unit volume. $f_{\mathrm{D,k}}$ is regarded as friction resistance per unit area of control part surface, and C_{D} is drag coefficient. $q_{\mathrm{m,k}}$ is regarded as mass flow rate of vapour -liquid phase transition in the control part. μ is viscosity coefficient.

According to the model, the droplets move horizontally at high speed. In this paper, the effects of surface tension, viscous force and volume expansion force are ignored. When one-dimensional flow equation of droplets is studied along the nozzle distance, the effects of buoyancy and gravity are not considered. Then momentum conservation equation of droplets is expressed as follows

$$\frac{\mathrm{d}\left(\rho_{\mathrm{k}}u_{\mathrm{k}}V_{\mathrm{k}}\right)}{\mathrm{d}\tau} + \frac{\mathrm{d}\left(\rho_{\mathrm{k}}u_{\mathrm{k}}u_{\mathrm{k}}V_{\mathrm{k}}\right)}{\mathrm{d}r} = q_{\mathrm{m,k}}u_{\mathrm{k}} - \frac{A\rho_{\mathrm{k}}C_{\mathrm{D}}u_{\mathrm{k}}^2}{2} \tag{18}$$

The momentum of liquid phase transition is transformed into vapour phase momentum by droplet spray flash. Because of small density variation, combining component and Eq.(19) gives the momentum conservation equation:

$$\frac{\rho_{\mathrm{d}} u_{\mathrm{d}} \mathrm{d}V}{\mathrm{d}\tau} + \frac{\rho_{\mathrm{d}} V \mathrm{d}u_{\mathrm{d}}}{\mathrm{d}\tau} + \frac{\mathrm{d}\left(\rho_{\mathrm{vap}} u_{\mathrm{I}}^2 V\right)}{\mathrm{d}r} = -\frac{A\rho_{\mathrm{d}} C_{\mathrm{D}} u_{\mathrm{d}}^2}{2} \tag{19}$$

Assumption $u_{\mathrm{I}} << u_{\mathrm{d}}$ and variation of droplet velocity with time is obtained based on Eqs.(12), (13) and (19):

$$\frac{\mathrm{d}u_{\mathrm{d}}}{\mathrm{d}\tau} = \frac{3}{D}\left(u_{\mathrm{d}} \frac{\mathrm{d}D}{\mathrm{d}\tau} + \frac{2\left(1-f_{\mathrm{m}}\right) h_{\mathrm{s}}^2}{\rho_{\mathrm{w}} \rho_{\mathrm{vap}} r^2} \left(\frac{\mathrm{d}t_{\mathrm{d}}}{\mathrm{d}\tau} \right)^2 - C_{\mathrm{D}} u_{\mathrm{d}}^2 \right) \tag{20}$$

4. 3. 3. Heat transfer

There is the energy conversion between heat energy and heat energy, heat energy and kinetic energy, kinetic energy and kinetic energy in the spray flash. Energy equation with phase transition is expressed as:

$$\frac{\partial}{\partial \tau}\left[\alpha_{\mathrm{k}} \rho_{\mathrm{k}} h_{\mathrm{k}}\right] + \vec{\nabla}\mathrm{g}\left[\alpha_{\mathrm{k}} \rho_{\mathrm{k}} h_{\mathrm{k}} u_{\mathrm{k}}\right] = -\alpha_{\mathrm{k}} p_{\mathrm{k}} \vec{\nabla}\mathrm{g}u_{\mathrm{k}} - \frac{\partial\left(\alpha_{\mathrm{k}} p_{\mathrm{k}}\right)}{\partial \tau} + \left(\vec{\nabla}\mathrm{g}\left(\alpha_{\mathrm{k}} \mu_{\mathrm{k}} u_{\mathrm{k}}\right) + G_{\mathrm{k}} + \Gamma_{\mathrm{k}} u_{\mathrm{k}} - f_{\mathrm{D,k}} + \alpha_{\mathrm{k}} \rho_{\mathrm{k}} g_{\mathrm{k}}\right) \vec{\nabla}\mathrm{g}u_{\mathrm{k}} \tag{21}$$

in which h_{k} is regarded as local enthalpy per unit mass of k-phase.

Similarly ignoring surface tension, viscous force, volume expansion force, buoyancy and gravity, energy conservation equation of droplet is established as:

$$\frac{\mathrm{d}\left(\rho_{\mathrm{k}} h_{\mathrm{k}} V_{\mathrm{k}}\right)}{\mathrm{d}\tau} + \frac{\mathrm{d}\left(\rho_{\mathrm{k}} u_{\mathrm{k}} h_{\mathrm{k}} V_{\mathrm{k}}\right)}{\mathrm{d}r} = -p_{\mathrm{k}} \frac{\mathrm{d}u_{\mathrm{k}}}{\mathrm{d}r} + q_{\mathrm{m,k}} u_{\mathrm{k}}^2 - \frac{A\rho_{\mathrm{k}} C_{\mathrm{D}} u_{\mathrm{k}}^3}{2} \tag{22}$$

The reduction of internal energy of liquid phase transition is equal to the increase of internal energy in vapour phase transition in control part. It is assumed that the steam of control part changes rapidly into saturated vapour corresponding to the environmental pressure. Combining component and Eq.(22) gives the energy conservation equation:

$$\frac{\rho_{\mathrm{d}} h_{\mathrm{d}} \mathrm{d}V}{\mathrm{d}\tau} + \frac{\rho_{\mathrm{d}} V \mathrm{d}h_{\mathrm{d}}}{\mathrm{d}\tau} + \rho_{\mathrm{vap}} u_{\mathrm{I}} A h_{\mathrm{vap}} = -p_{\mathrm{d}} \frac{\mathrm{d}u_{\mathrm{d}}}{\mathrm{d}r} - \frac{A\rho_{\mathrm{d}} C_{\mathrm{D}} u_{\mathrm{d}}^3}{2} \tag{23}$$

Application of approximate formula between temperature and specific enthalpy.

$$h_{\mathrm{d}} = c_{\mathrm{d}} t_{\mathrm{d}} \tag{24}$$

in which C_{d}=4.196 kJ • $\mathrm{kg}^{-1}\mathrm{K}^{-1}$.

Meanwhile vapour is calculated as ideal gas. Variation of droplet temperature with time is obtained based on Eqs.(12), (13) , (23)and (24):

$$\frac{\mathrm{d}t_\mathrm{d}}{\mathrm{d}\tau}=-\frac{3}{c_\mathrm{d}D+\dfrac{21\left(1-f_\mathrm{m}\right)h_\mathrm{s}R}{\rho_\mathrm{w}rM}\left(273.15+t_\mathrm{d}\right)}\left(\frac{\left(1-f_\mathrm{m}\right)p_\mathrm{d}}{\rho_\mathrm{w}}\frac{\mathrm{d}D}{\mathrm{d}\tau}+C_\mathrm{D}u_\mathrm{d}^3+c_\mathrm{d}t_\mathrm{d}\frac{\mathrm{d}D}{\mathrm{d}\tau}\right) \tag{25}$$

4. 4. Solution result

Giving initial liquid temperature, Δp and f_m, the one-dimensional distribution of droplets size along the injection direction is calculated by the governing Eq.(26).

$$\begin{cases}\dfrac{\mathrm{d}D}{\mathrm{d}\tau}=\dfrac{2\left(1-f_\mathrm{m}\right)h_\mathrm{s}}{\rho_\mathrm{w}r}\dfrac{\mathrm{d}t_\mathrm{d}}{\mathrm{d}\tau}\\ \dfrac{\mathrm{d}u_\mathrm{d}}{\mathrm{d}\tau}=\dfrac{3}{D}\left(u_\mathrm{d}\dfrac{\mathrm{d}D}{\mathrm{d}\tau}+\dfrac{2\left(1-f_\mathrm{m}\right)h_\mathrm{s}^2}{\rho_\mathrm{w}\rho_\mathrm{vap}r^2}\left(\dfrac{\mathrm{d}t_\mathrm{d}}{\mathrm{d}\tau}\right)^2-C_\mathrm{D}u_\mathrm{d}^2\right)\\ \dfrac{\mathrm{d}t_\mathrm{d}}{\mathrm{d}\tau}=-\dfrac{3}{c_\mathrm{d}D+\dfrac{21\left(1-f_\mathrm{m}\right)h_\mathrm{s}R}{\rho_\mathrm{w}rM}\left(273.15+t_\mathrm{d}\right)}\left(\dfrac{\left(1-f_\mathrm{m}\right)p_\mathrm{d}}{\rho_\mathrm{w}}\dfrac{\mathrm{d}D}{\mathrm{d}\tau}+C_\mathrm{D}u_\mathrm{d}^3+c_\mathrm{d}t_\mathrm{d}\dfrac{\mathrm{d}D}{\mathrm{d}\tau}\right)\\ \dfrac{\mathrm{d}x}{\mathrm{d}\tau}=u_\mathrm{d}\end{cases} \tag{26}$$

Evaporation rate (ψ) represents the intensity of the spray flash and is expressed as Eq.(27). The relative errors shown in Fig.9 all suggest that the calculated result of this model are in good agreement with experimental results.

$$\psi\left(x\right)=\frac{\Delta m_\mathrm{d}}{m_{\mathrm{d},0}}=1-\left[\frac{D\left(x\right)}{D_0}\right]^3 \tag{27}$$

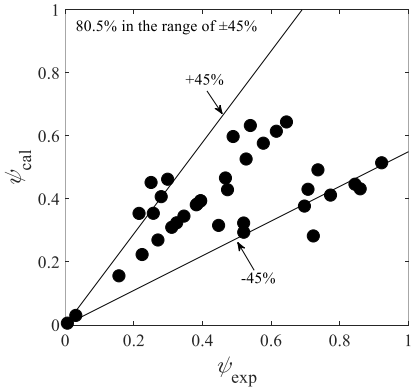

Fig. 9: Error distribution of ψ.

5. Conclusion

In this paper, experimental study on evaporation properties under Δp, ΔT, f_m and x during spray flash of aqueous NaCl solution. The velocity field is measured by the high-speed camera and image registration. The droplet size is measured by Malvern. The conclusion include:

a. Velocity increases with rising Δp or ΔT, and decreases with rising f_m. The droplet size decreases with rising Δp or x, and decreases with rising ΔT or f_m.

b. Differential pressure increases cause initial kinetic energy increases deepens the atomization.

c. Superheat is driving force of flash, ΔT sharply promote droplets nucleation, atomization and evaporation.

d. Mass fraction increases cause surface tension increases that restrain spray flash.

e. On basis of these results, a one-calculation model for spray flash was set up. The evolution of droplet size/velocity/ temperature could be well computed from given evolution of spray flash pressure and other necessary initial conditions.

Nomenclature

A, area (m^2)
C_D, drag coefficient (-)
c, specific heat (kJ kg^{-1} K^{-1})
D or D_{32}, droplet size (μm)
f_m, mass fraction (-)
h_s, surface heat transfer coefficient (kW m^{-3} K^{-1})
Ja, Jakob number
k, thermal conductivity of phase k
m, mass (kg)
Nu, Nusselt number
p, pressure (MPa)
r, latent heat (kJ kg^{-1})
Re, Reynolds number
t, temperature (℃)
u, velocity (m s^{-1})
V, volume (m^3)
x, axial distance (mm)

Greek symbols

ΔT, superheat (K)
ρ, density (kg m^{-3})
τ, time (s)
ψ, evaporation rate (-)
Γ, mass of phase transition (kg)

Subscript

vap, vapor
I, vapour diffusion

Acknowledgements

This work is supported by National Key R&D Program of China (2018YFB0604303), and by National Natural Science Foundation of China (51976162).

References

[1] D H Kim, “A review of desalting process techniques and economic analysis of the recovery of salts from retentates,” *Desalination*, vol. 270, no. 2011, pp. 1-8.

[2] S Chantasiriwan, “Distribution of juice heater surface for optimum performance of evaporation process in raw sugar manufacturing [J],” *Journal of Food engineering*, vol. 195, no. 2017, pp. 21-30.

[3] Wenlong Chen, Weiwei Zhang, Hua Chen et al., “Spray cooling and flash evaporation cooling: The current development and application[J],” *Renewable and sustainable energy review*, vol. 55, no. 2016, pp. 614-628.

[4] E Sher, T B Kohany, A Rashkovan, “Flash-boiling atomization[J],” *Progress in Energy and Combustion Science*, vol. 34, no. 2008, pp. 417-439.
[5] O.Miyatake, T. Tomimura, Y. Ide, et al., “An experimental study of spray flash evaporation[J],” *Desalination*, vol. 36, no. 2, pp. 113-128, 1981.
[6] Y. Ikegami, H. Sasaki, T. Gouda, et al., “Experimental study on a spray flash desalination (influence of the direction of injection) [J],” *Desalination*, vol. 194, no. 2006, pp. 81-89.
[7] A. H. Araghi, M. Khiadani, M. H. Sadafi, “A numerical model and experimental verification for analyzing a new vacuum spray flash desalinator utilizing low grade energy[J],” *Desalination*, vol. 413, no. 2017, pp. 109-118.
[8] D. Zhang, J. J. Yan, B. C. Zhao, J. T. Feng. “Experimental study on energy conversion efficiency during static flash of aqueous NaCl solution[J].” *International Journal of Heat and Mass Transfer*, vol. 83, 2015.
[9] H. H. Wang, D. Zhang, Z. C. Niu, H. Wu. “Measurement of Atomization Velocity Field in Spray Flash [J],” *Journal of Engineering Thermophysics*, vol. 40, no. 10, 2019.
[10] R. J. Moffat, “Contributions to the theory of single-sample uncertainty analysis[J],” *Journal of Fluid Engineering*. vol. 104, no. 1982, pp. 250-260.